ACS OMEGA

http://pubs.acs.org/journal/acsodf

Article

Neurodevelopmental Toxicity of Polystyrene Nanoplastics in *Caenorhabditis elegans* and the Regulating Effect of Presenilin

Qianyun Liu,[§] Chunxiang Chen,[§] Mengting Li, Jia Ke, Yichen Huang, Yuefeng Bian, Shufen Guo, Yang Wu, Yan Han,* and Mingyuan Liu*

Cite This: *ACS Omega* 2020, 5, 33170−33177

Read Online

ACCESS | Metrics & More | Article Recommendations

ABSTRACT: As one of the most widely used materials, plastic polymer fragments can abrasively degrade into microplastic (MP) and smaller nanoplastic (NP) particles. The present study aimed to investigate the influence of particle size on neurodevelopmental toxicity induced by polystyrene nanoplastics (PS-NPs) in *Caenorhabditis elegans* and to explore the underlying potential mechanism. *C. elegans* were exposed to different concentrations of PS-NPs with various sizes (25, 50, and 100 nm) for 72 h. Our results showed that all of these PS-NPs could dose-dependently induce an increase in reactive oxygen species production and mitochondrial damage in *C. elegans*, resulting in inhibition of body length, head thrashes, body bending, and dopamine (DA) contents. A weaker neurotoxicity was found in 25 nm PS-NPs compared to 50 and 100 nm PS-NPs, which might be due to preferential cellular distribution and greater polymerization capability of the smaller particles. In addition, all these PS-NPs could induce lipofuscin accumulation and apoptosis independent of particle size, suggesting that oxidative damage and mitochondrial dysfunction may not be the only way responsible for NP-induced neurotoxic effects. Furthermore, the mutant test targeting two presenilin genes (*sel-12* and *hop-1*) showed that *sel-12* and *hop-1* were involved in regulation of PS-NP-induced neurodevelopmental toxicity and mitochondrial damage. In conclusion, PS-NPs could induce neurodevelopmental toxicity dependent on particle sizes mediated by mitochondrial damage and DA reduction. Enhanced expression of presenilin plays a role in PS-NP-induced oxidative stress and neurodevelopmental toxicity.

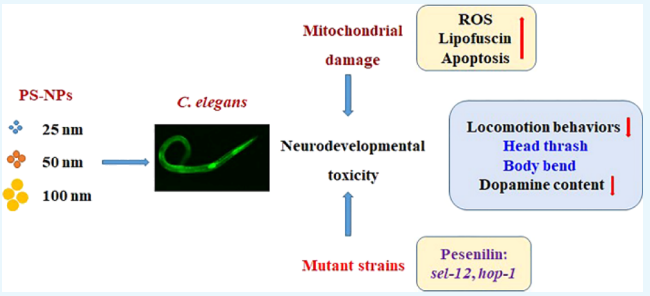

1. INTRODUCTION

The plastic polymer is one of the most world-widely used materials, and plastic polymer fragments can be abrasively degraded into microplastic particles (MPs, with a diameter smaller than 5 mm) and smaller nanoplastics (NPs, with a diameter smaller than 100 nm) in environments. In addition, some primary MPs originate from the production processes of preproduction pellets, synthetic textiles, cosmetics, and personal care products.[1,2] Now, MPs have been ubiquitously detected in sediments, oceans, rivers, sewages, soil, and various marine species including fish, bivalves, birds, mammals, and invertebrates,[3,4] with average concentrations ranging from ng/L to μg/L in aquatic and terrestrial environments.[5] The large specific surface area and excellent adsorption capability of MPs make them serve as good vectors for exogenous toxicants, including various metals and organic pollutants, which would further intensify their influences on the ecological environment.[6] Moreover, MPs and NPs could transfer through the food chain and eventually enter organisms through the skin, respiratory tract, and digestive tract.[2,7,8] It has been reported that plastic particles ($\lesssim$0.3 μm) could reach and accumulate in the liver, spleen, and lymphatic systems of rodents.[9] A surveying on eight healthy volunteers from Europe and Asia showed that up to nine types of MPs including polypropylene and polyethylene terephthalate have been detected in human stool samples.[10] Recently, research studies have confirmed that MPs could break through the blood−brain barrier (BBB) and accumulate in the brain tissue of fish.[11−13]

Previous studies have reported adverse effects of these small plastic particles on marine organisms, invertebrates, and mammals. The central nervous system (CNS) was identified as an important target for the toxic effects of MPs.[13,14] Exposure to MPs (1−5 μm) could cause damages to the motor nerve in European seabass through inhibition of acetylcholinesterase (AChE) activity (a representative biomarker for neurotoxicity).[15] Polystyrene microplastics (PS-MPs, 100 μm) also induced significant nuclear alterations, DNA damage, and

Received: October 2, 2020
Accepted: November 25, 2020
Published: December 18, 2020

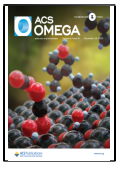

https://dx.doi.org/10.1021/acsomega.0c04830
ACS Omega 2020, 5, 33170−33177

reduction of AChE activity in the gills of Mediterranean mussels (*Myetilus galloprovincialis*).[16] Furthermore, exposure of PS-MPs (5 and 20 μm) also significantly reduced the AChE activity in mice liver, suggesting the potential neurotoxicity in mammals.[17]

Generally, accumulation and toxic potential of plastic debris in the organism tissues increase when plastic fragments into smaller particles such as microplastics (<1 mm) or nanoparticles (<100 nm).[18] Presently, several studies investigated the neurotoxicity of NPs in aquatic organisms. The decrease in AChE activity and induction of oxidative stress were observed after polystyrene nanoplastic (PS-NP) exposure in brine shrimp (*Artemia fransiscana*) and adult tilapia fish *Oreochromis niloticus*, indicating the neurotoxic potency of PS-NPs.[12,19] PS-NPs (50 nm) detected in the brain of adult zebrafish were reported to cause upregulation of CNS myelin basic protein and inhibition of AChE activity.[20] Moreover, Mattsson *et al.* reported that *Daphnia magna* exposed to amino (ANP)-modified NPs (53 nm) showed weight decrease, water loss, and NP accumulation in the brain tissue, resulting in a slower feeding rate and lower hunting efficiency than controls.[21]

However, the underlying potential mechanism of NP-induced neurotoxicity is poorly understood until now. There were only a few toxicological research studies which indicated that oxidative stress and subsequent DNA damage were associated with the neurotoxicity induced by NPs.[13,22,23] *Caenorhabditis elegans* has many excellent advantages as an *in vivo* model organism for neurotoxicity evaluation, including the short development cycle from egg to adult, short life span between 2 and 3 weeks, and easy handling with translucent body.[24] In addition, approximately 60−80% of worm genes have the corresponding human orthologs, such as neurodegenerative disease-related proteins amyloid precursor protein (APP) and microtubule-associated Tau protein. Furthermore, *C. elegans* lacks a functional BBB, making neurotoxins easy to spread in the nervous system.[25] In this study, *C. elegans* were exposed to different sizes of PS-NPs (25, 50, and 100 nm), and the impact of NP size on the neurotoxicity was investigated. Furthermore, the mutant nematode strains were applied to explore the potential toxicological mechanism.

2. RESULTS AND DISCUSSION

2.1. Effect of PS-NPs on Growth and Locomotion Deficits in *C. elegans*. Various factors such as particle size, material type, exposure concentration, and exposure duration have been confirmed as the influencing factors on the neurotoxicity of MPs and NPs. Among them, particle size is assumed to be a crucial factor correlated with toxicity. However, the precise manner of particle size affecting the biological process is still unknown. The results of Mattsson *et al.* reported that positively charged ANP-modified PS-NPs (from 52 to 330 nm) could reduce the survival rate of Daphnia, penetrate the BBB in fish, and cause behavioral disorders dependent on size.[21] In this study, different sizes of PS-NPs (25, 50, and 100 nm) were applied to investigate the biological effect and locomotion behavior in *C. elegans* in terms of body length, head thrashes, and body bending. The experimental concentrations from 10 to 100 μg/L were selected in this study according to our pre-experiment. As shown in Figure 1A, after treatment of PS-NPs, the body length of *C. elegans* decreased in a dose-dependent manner. The larger particle (50 and 100 nm) seemed to have higher

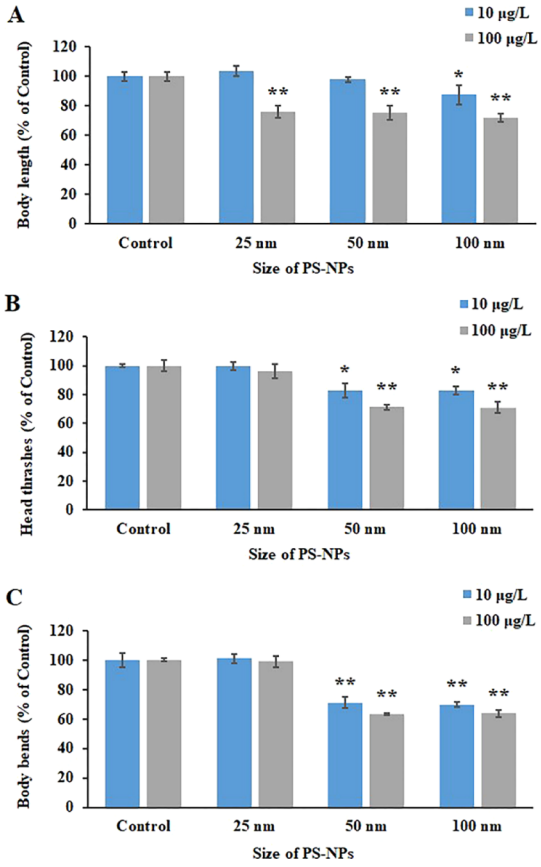

Figure 1. Effect of different sizes of PS-NPs on growth and locomotion behavior of *C. elegans*. *C. elegans* were treated with 10 and 100 μg/L PS-NPs particles (25, 50, and 100 nm) for 72 h, and then, (A) body length, (B) head thrashes, and (C) body bends were measured, as described in the Materials and Methods. The control group was treated with K^+ medium alone. *p < 0.05 and **p < 0.01, compared with control groups.

efficiency than 25 nm particles on inhibition of body growth, although the difference is of no statistical significance. Consistently, the locomotion behavior assays also indicated that *C. elegans* had obvious locomotion deficits after exposure to 50 and 100 nm PS-NPs, but not 25 nm PS-NPs (Figure 1B,C). In the groups of 10 and 100 μg/L 50 nm PS-NPs, the frequency of head thrashes and body bends reduced by 17.2 and 28.8, and 29.0 and 37.0% as compared to the control group, respectively. Similarly, PS-NPs of 100 nm (10 and 100 μg/L) caused reduction of head thrashes and body bends by 17.4 and 29.2, and 30.3 and 36.3%, respectively. These results suggest that the toxic severity of plastic particles with the diameter in the nanometer range (<100 nm) was inversely related to particle sizes.

Based on research of the simulated biomimetic heterogeneous membrane interface, small NP particles (<200 nm) dominantly localized in the ordered phase, whereas larger particles mainly accumulated in the fluidic disordered phase, indicating that different sizes of NPs had preferential compatibility with the two-phase liposomes of the cell surface.[26] In the previous study on NPs and MPs with diameters ranging from 500 to 5.0 μm, the most significant toxic effects were found in the groups of 500 and 1000 nm MP particles. The smaller 100 nm NPs and larger 2 and 5 μm MPs had almost equivalent neurotoxicity in *C. elegans*, which was

https://dx.doi.org/10.1021/acsomega.0c04830
ACS Omega 2020, 5, 33170−33177

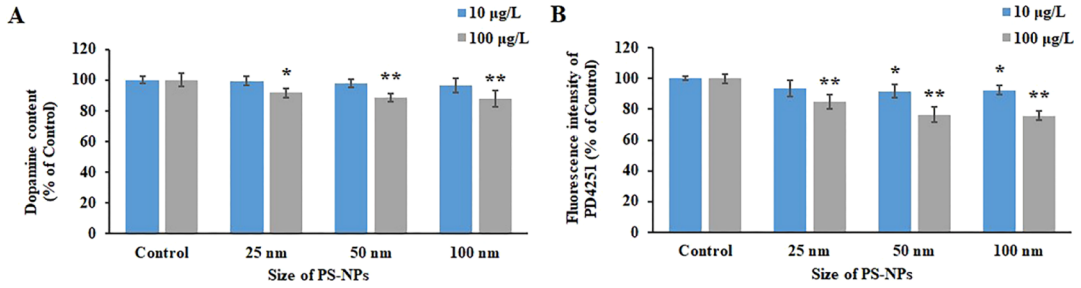

Figure 2. Dopaminergic loss and mitochondrial damage induced by PS-NPs in *C. elegans*. *C. elegans* were treated with 25, 50, and 100 nm PS-NP particles (10 and 100 μg/L) for 72 h, and then, (A) DA content and (B) mitochondrial damage were examined with fluorescence detection, as described in the Materials and Methods. The control group was treated with K^+ medium alone. *$p < 0.05$ and **$p < 0.01$, compared with control groups.

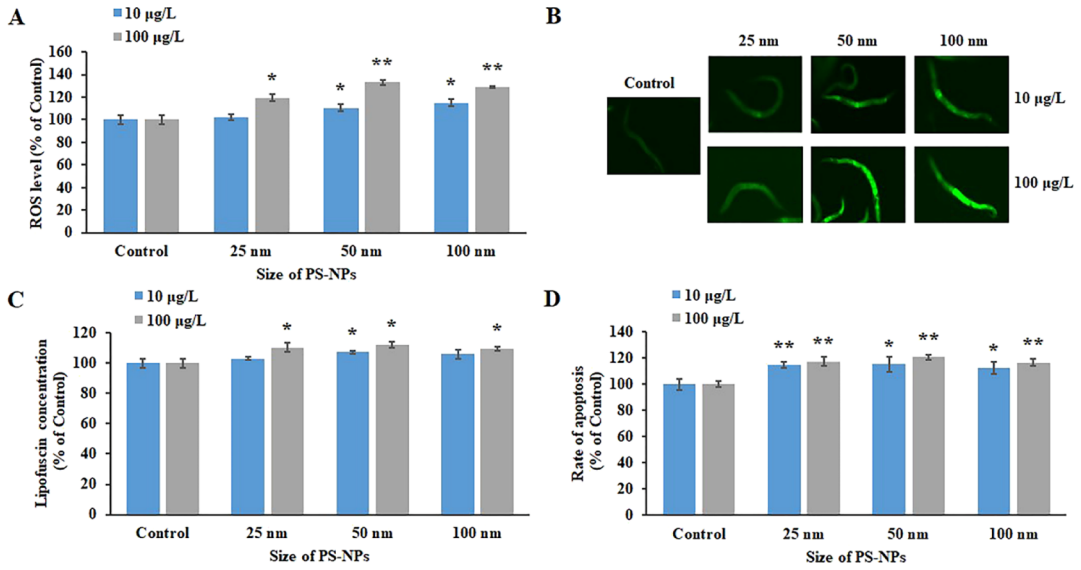

Figure 3. Oxidative damage and apoptosis induced by NPs in *C. elegans*. *C. elegans* were treated with 10 and 100 μg/L PS-NP particles with different sizes (25, 50, and 100 nm) for 72 h, and then, the (A) ROS level, (C) lipofuscin accumulation, and (D) apoptosis were detected, as described in the Materials and Methods. (B) Representative images of ROS production. *$p < 0.05$ and **$p < 0.01$, compared with control groups.

weaker than that of 500 and 1000 nm MP particles.[27] It was reported that monodisperse nano-PS could easily cross the biological barriers, but the agglomerate nanoparticles would be physically blocked from the cell membrane.[28] Our results also showed that PS-NPs less than 200 nm could quickly penetrate and integrate into cell membranes and consequently cause neurotoxicity. As for the weaker toxic effects of 25 nm PS in *C. elegans* observed in this study, we speculate that it might be because of the easier polymerizing characteristic of these smaller nanoparticles.

2.2. Dopaminergic Loss and Mitochondrial Damage Induced by Different Sizes of PS-NPs in *C. elegans*. NP exposure was reported to cause neurotoxicity manifested as alterations of neurotransmitter and neuronal behavior disorders.[13] As a major catecholamine neurotransmitter in the brain, dopamine (DA) participates widely in neurobiological processes. Dysregulation of the DA balance is a crucial pathogenic mechanism of Parkinson's disease, schizophrenia, Tourette syndrome, cognitive disfunction, and so forth.[29] Recently, DA changes following exposure of MPs have been reported in bivalves and fish.[20,30] Using a human three-dimensional *in vitro* model of early CNS PAX6(+) precursor cells derived from the embryonic stem cell, polyethylene NPs (33 nm) were found to accumulate in dopaminergic neurons and interfere with expression of the Notch pathway genes.[31] In this study, to determine the developmental neurotoxicity (DNT) of PS-NPs, transgenic *C. elegans* strain BZ555 was treated with different concentrations of PS-NPs, and the DA content was examined in the fluorescently labeled dopaminergic neuron. As shown in Figure 2A, compared with the control groups, there was no effect on the DA content after 10 μg/L PS-NP exposure. However, under the 100 μg/L NPs treatment, DA content was downregulated by 25, 50, and 100 nm NPs with 8.2, 11.5, and 12.2% reduction, respectively ($p < 0.05$). The lower frequency of head thrashes and body bending (Figure 1B,C) and reduction of DA content (Figure 2A) indicated the DNT induced by PS-NPs.

Mitochondrial dysfunction has been proposed as an important mechanism for substantia nigra dopaminergic neurodegeneration.[32] To characterize the mechanisms of DNT induced by PS-NPs, a transgenic PD4251 strain with the green fluorescent protein (GFP)-labeled mitochondria was applied to examine the mitochondrial damage. As shown in Figure 2B, the reduced fluorescence signal compared with control groups indicated mitochondrial damage induced by PS-NPs (Figure 2B). Consistent with DA assay, the biological effect of 25 nm PS-NPs was weaker in inducing mitochondrial damage than that of larger size PS-NPs. Quantized results

https://dx.doi.org/10.1021/acsomega.0c04830
ACS Omega 2020, 5, 33170−33177

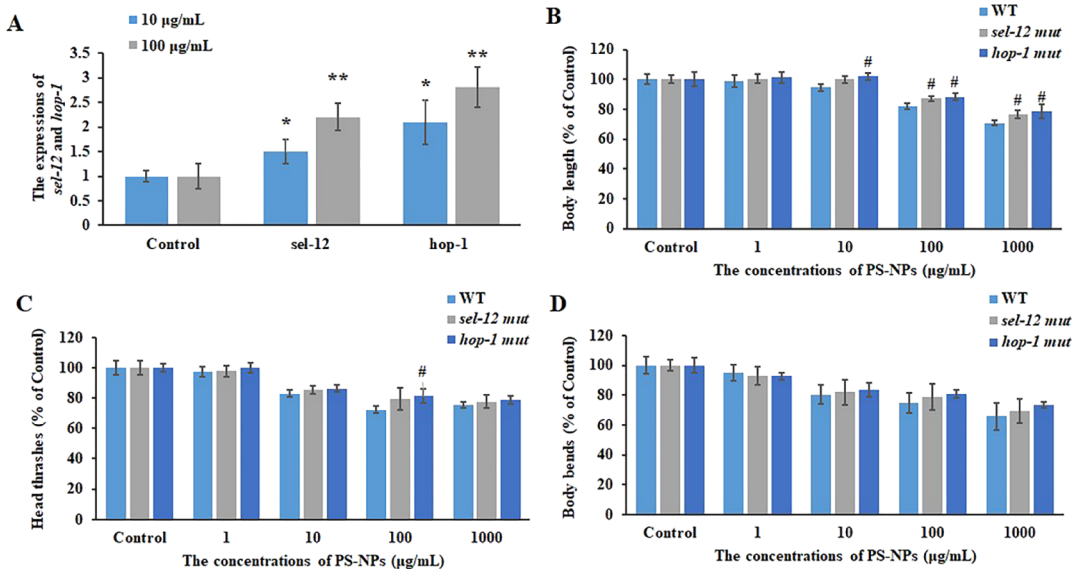

Figure 4. Regulation of *sel-12* and *hop-1* on neurodevelopmental toxicity induced by NPs. WT, *sel-12* (AR171), and *hop-1* (LA62) mutant strains were treated with 1, 10, 100, and 1000 μg/L 50 nm PS-NP particles for 72 h, and then, (A) the expressions of *sel-12* and *hop-1*, (B) body length, (C) head thrashes, and (D) body bends were detected. *$p < 0.05$ and **$p < 0.01$, compared with control groups; #$p < 0.05$, compared with WT groups.

showed that 10 and 100 μg/L 100 nm PS-NPs caused significant reductions of fluorescence intensity by 7.5 and 24.2%, respectively ($p < 0.05$). Previously, it was reported that NH (2)-labeled PS-NPs (60 nm) could induce mitochondrial damage and ATP depletion in human epithelial (BEAS-2B) cells.[33] ANP-modified PS-NP (50 and 100 nm) exposure resulted in mitochondrial disruption and release of cytochrome C in primary human alveolar macrophages, primary human alveolar type 2 epithelial cells, and the human alveolar epithelial type I-like cell (TT1).[34] These abovementioned findings suggest that mitochondrial damage might be one of the important mechanisms by which PS-NPs induced neurodevelopmental toxicity.

2.3. Oxidative Stress and Apoptosis Induced by PS-NPs in *C. elegans*. Mitochondria are important organelles involved in the intracellular Ca^{2+} signaling pathway, ATP production, maintenance of membrane stability, and reactive oxygen species (ROS) balance. Excessive production of active oxygen in the mitochondria is responsible for various physiology disorders. In the gills, PS-MPs induced a consistent increase in SOD and glutathione-*S*-transferase activity, and then, AChE and lipid peroxidation (LPO) activity reduced subsequently.[35] Treatment of PS-MPs (5 and 20 μm) also triggered oxidative stress in mice liver tissue as evidenced by increased glutathione peroxidase and SOD and decreased catalase (CAT).[17] To examine the oxidative stress response in *C. elegans*, ROS production induced by PS-NP particles was detected with a 2′,7′-dichlorodihydrofluoresceindiacetate (DCFH-DA) assay. As shown in Figure 3A, exposure of 10 μg/L 25 nm PS-NPs had no obvious effect on ROS production, while 100 μg/L 25 nm PS-NPs did increase the intracellular ROS level. Compared to the control group, both 10 and 100 μg/L 50 nm PS-NP exposure resulted in a significant increase in ROS production by 10.5 and 33.3%, respectively. For 10 and 100 μg/L 100 nm PS-NPs, the level of ROS levels increased by 14.9 and 28.9%, respectively.

Increased lipofuscin and LPO are generally considered to be crucial biomarkers for cellular damages induced by oxidative stress.[36] As shown in Figure 3B, lower concentrations of PS-NPs (10 μg/L) had only slight effects on lipofuscin induction, and higher concentrations of (100 μg/L) PS-NPs (25, 50, and 100 nm) could significantly stimulate the lipofuscin levels ($p < 0.05$) by 10.3, 12.2, and 9.3%, respectively, as compared with the control group. Furthermore, the acridine orange (AO) staining results showed that 25, 50, and 100 nm PS-NPs significantly induced an average apoptosis rate of 12.4−20.7% (Figure 3C). The elevated ROS production, lipofuscin accumulation, and apoptosis induction indicated oxidative damages *via* mitochondrial dysfunction and might play a role in biological effects after NP exposure, which was consistent with the results of previous studies. In the study of Qu *et al.*, ANP-modified PS-NPs induced apoptosis and DNA damages through oxidative stress in *C. elegans*.[37] The accumulation of 50 nm ANP-modified PS-NPs in lysosomes could lead to release of cathepsins into the cytosol, which ultimately propagated the mitochondrial damages and subsequent activation of apoptosis in human astrocytoma cells.[38]

Meanwhile, it was found that different sizes of PS-NPs had no differential effect in inducing lipofuscin and apoptosis, indicating that mitochondrial dysfunction and subsequent oxidative damage might not be the exclusive mechanism responsible for NP-induced neurotoxicity. According to results of literature reviewing, lysosomal destabilization and inflammation are also involved in DNT induced by NP exposure.[39,40]

2.4. Regulation of Presenilin on Neurodevelopmental Toxicity Induced by PS-NPs. Presenilin, mainly distributed in the endoplasmic reticulum (ER) and mitochondria, is closely related to mitochondrial toxicity and mitochondrial phagocytosis.[41] In mammals, presenilin-1 (PS1) and -2 (PS2) constitute the catalytic components of the γ-secretase complex, which processes APP to produce amyloid-β.[42] It is reported that mutation of presenilin genes is associated with the onset of Alzheimer's disease, dementia, and Parkinson's disease.[43] In *C. elegans*, the presenilin genes *sel-12* or/and *hop-1* constitute the catalytic subunit of the γ-secretase proteolytic enzyme, mediating activation of the Notch

https://dx.doi.org/10.1021/acsomega.0c04830
ACS Omega 2020, 5, 33170−33177

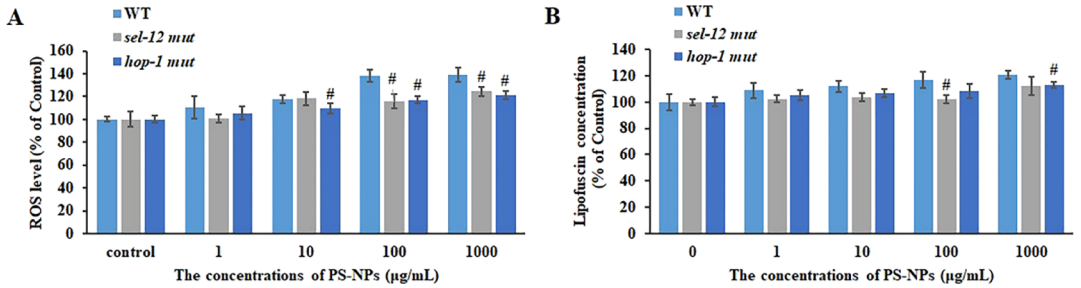

Figure 5. Regulation role of *sel-12* and *hop-1* on oxidative damage induced by NPs. WT, *sel-12* (AR171) and *hop-1* (LA62) mutant strains were treated with 1, 10, 100, and 1000 μg/L 50 nm PS-NPs particles for 72 h, and then, (A) ROS production and (B) lipofuscin concentration were detected. #$p < 0.05$, compared with WT groups.

pathway.[44] *Sel-12* can induce apoptosis under oxidative stress in *C. elegans* through a mitochondrial pathway *via* abnormal calcium release from the ER.[45] Mutation of *hop-1* can attenuate the survival reduction, motor deficits, and dopaminergic degeneration in *C. elegans* induced by rotenone or paraquat through mitochondria-associated mechanisms.[46]

Based on the abovementioned experimental results, 50 nm PS-NPs were selected for subsequent experiments of the presenilin gene. As shown in Figure 4A, real time-quantitative polymerase chain reaction (RT-qPCR) results revealed that 50 nm PS-NPs could significantly stimulate the expression of *sel-12* and *hop-1*, indicating involvement of *sel-12* and *hop-1* in neurodevelopmental toxicity induced by PS-NPs. To clarify the role of presenilin, nematode strains AR171 (*sel-12* mutant) and LA62 (*hop-1* mutant) were further applied in mutant experiment. As displayed in Figure 4B, compared with the wild-type (WT) *C. elegans*, both AR171 and LA62 could partially reverse the decrease in body length induced by PS-NPs exposure. In *sel-12* mutant groups, the body length of *C. elegans* after 100 or 1000 μg/mL NP exposure increased by 6.3 or 8.5% compared to that of WT groups, respectively. For *hop-1* mutant groups, the body length of the 10, 100, or 1000 μg/mL NP groups increased by 7.6, 7.5, and 11.1%, respectively ($p < 0.05$, Figure 4B). Similarly, the inhibitory effect on movement behavior caused by the 50 nm PS-NP was alleviated by mutants of *sel-12* and *hop-1* (Figure 4C,D). In addition, the *sel-12* mutant could also alleviate the increase in ROS level and lipofuscin accumulation caused by 100 and 1000 μg/mL PS-NP treatment, with 16.2 and 10.6, and 12.6 and 7.1% reduction, respectively (Figure 5A,B). Compared to the WT groups, the ROS production and lipofuscin concentration in *hop-1* mutant groups after 100 and 1000 μg/mL PS-NP treatment reduced by 15.2 and 13.0, and 7.3 and 6.1%, respectively (Figure 5A,B). These results suggested that presenilin genes *sel-12* and *hop-1* play a regulatory role in the neurotoxicity induced by PS-NPs.

3. CONCLUSIONS

Different sizes (25, 50, and 100 nm) of PS-NPs were used in the present study to treat *C. elegans*, aiming to investigate the impact of particle size on PS-NP-induced neurodevelopmental toxicity. Measurement of body length, head thrashes, and body bending showed that PS-NPs exerted significant neurodevelopmental toxic effects in *C. elegans* in a dose-dependent manner. The severity of neurotoxicity was inversely related to particle sizes, which may be because of preferential cellular distribution and better polymerizing characteristic of smaller nanoparticles (25 nm). Similarly, PS-NPs dose-dependently induced ROS production, mitochondrial damage, and DA reduction in *C. elegans*, which was also influenced by particle sizes. In addition, PS-NP-induced lipofuscin accumulation and apoptosis were independent of particle size, suggesting the existence of other toxicological mechanisms besides the mitochondrial pathway. Furthermore, results of the mutant test showed that enhanced expression of *sel-12* and *hop-1* were involved in regulation of PS-NP-induced oxidative stress, mitochondrial damage, and neurodevelopmental toxicity in *C. elegans*.

4. MATERIALS AND METHODS

4.1. Chemicals and Reagents. PS-NP beads (5% w/v) of three different sizes with good monodispersity were purchased from Janus New Materials Co. (Nanjing, China). AO and DCFH-DA were purchased from Beyotime Biotechnology (Shanghai, China). TRIzol reagents were obtained from Invitrogen (CA, USA). A Fast Quant RT kit was obtained from Tian Gen (Beijing, China). The SYBR Green PCR kit was purchased from Roche (Basel, Switzerland). All other reagents of analytical grade used in this study were purchased from Sigma (MO, USA).

4.2. Maintenance and Synchronization of *C. elegans*. All strains of *C. elegans* listed in Table 1 were purchased from the Caenorhabditis Genetics Center (University of Minnesota, Minneapolis, MN, USA) and maintained in the standard nematode growth medium (NGM containing: NaCl 50 mM, peptone 2.5 g/L, agar 17 g/L, potassium phosphate 25 mM, $CaCl_2$ 1 mM, $MgSO_4$ 1 mM, and cholesterol 1.5 g/L). Nematodes were cultured on NGM agar plates seeded with *Escherichia coli OP50* at 20 °C. For synchronization, gravid adult nematodes were treated with Clorox solution (5% NaOCl/1 M NaOH = 2:1, v/v) for 10 min, and then, the nematode suspensions were centrifuged at 2200 rpm for 2 min. The collected embryos were maintained on new NGM agar plates with *E. coli OP50* at 20 °C.

Table 1. *C. elegans* Strains Used in This Study[a]

strain name	genotype description
WT	Bristol wild type
BZ555	transgenic GFP in DA neurons
PD4251	transgenic mitochondrial GFP
AR171	*sel-12* mutant
LA62	*hop-1* mutant

[a]Note: GFP refers to green fluorescent proteins and DA refers to dopamine.

4.3. Exposure Test with PS-NP Particles. According to the results of our preliminary experiments, the stock solution

https://dx.doi.org/10.1021/acsomega.0c04830
ACS Omega 2020, 5, 33170−33177

(1 mg/mL) of PS-NP particles was diluted using K^+ medium (NaCl 50 mM, KCl 32 mM, $MgSO_4$ 3 mM, $CaCl_2$ 3 mM, and cholesterol 1.5 g/L) into different working concentrations of 1, 10, 100, and 1000 μg/L. Nematodes at the L1 larvae period were exposed to PS-NP particles for 72 h. The control group was treated with K^+ medium alone. Each experimental group included three parallels. After PS-NP exposure, nematodes were washed three times with K medium (NaCl 50 mM and KCl 32 mM) to prepare samples for toxicity evaluation.

4.4. Measurement of Growth and Locomotion Behaviors. Synchronized WT or transgenic nematodes at the L1 larval stage were exposed to PS-NPs at 20 °C for 72 h. After exposure, nematodes were immobilized by heat, and the body length of nematodes was measured with a microscope (Olympus BX51, Japan) and analyzed with ImageJ software.[47]

Head thrash and body bending were utilized as evaluating parameters for locomotion behaviors of nematodes. A head thrash is defined as one swing of nematode body, and a body bending refers to crawling of one wavelength.[48] After PS-NP exposure, *C. elegans* was transferred to the surface of fresh NGM, and the frequency of head thrash and body bending within 20 s were counted under a microscope (Olympus BX51, Japan). For each treatment group, at least 20 nematodes were randomly picked and examined from three independent experiments.

4.5. Detection of DA Content. The DA neurons of *C. elegans* BZ555 strain (dat-1:GFP) were labeled with a GFP, and the fluorescence intensity refers to the DA content in nematodes.[49] In brief, the BZ555 strain was exposed to PS-NPs for 72 h, then transferred to agar-padded (2%) slides, and anesthetized with levamisole solution (60 μm). The fluorescent images of immobilized nematodes were photographed with a microscope (Olympus BX51, Japan) and analyzed with ImageJ software.[50] At least 20 nematodes were randomly picked and examined for each concentration treatment.

4.6. Observation on Mitochondria-Associated Membranes. The GFP reporter *C. elegans* strain PD4251 strain contains both nuclear gfp-lacZ and mitochondrial gfp,[51] and interference of GFP signals in the cytoplasm reflects the alterations of mitochondria-associated membranes. In this study, the PD4251 strain was treated with different sizes of PS-NPs for 72 h and then transferred to agar-padded (2%) slides. Anesthesia, GFP fluorescence observation, and fluorescent intensity analysis were conducted as described above.

4.7. Oxidative Stress and Lipofuscin Analysis. Active oxygen radicals in *C. elegans* oxidize the nonfluorescent DCFH to fluorescent DCF, which can be used to determine the content of ROS. After treatment of PS-NPs for 72 h, nematodes were incubated with 10 μm of DCFH-DA diluted with K medium in the dark for 2 h. Then, nematodes were anesthetized with 60 μm of levamisole solution, and the fluorescence intensity was measured using the multifunctional microplate reader with an excitation wavelength at 488 nm and emission filter at 510 nm.[52−54]

Lipofuscin accumulation is used as a biomarker for cellular damage induced by oxidative stress.[36] For lipofuscin assessment, nematodes were exposed to PS-NPs for 72 h and washed three times with K medium. Then, nematodes were transferred to agar-padded (2%) slides and treated with 60 μm of levamisole solution. Images of immobilized nematodes were photographed with a microscope (Olympus BX51, Japan) and analyzed with ImageJ software.[50] At least 20 nematodes were randomly picked and examined for each concentration treatment.

4.8. AO Staining Analysis. The permeable dye AO can penetrate the live cell membranes and stain cell nuclei with uniform green fluorescence. For apoptotic cells, AO stains nuclei with dense and bright green dots because of the presence of apoptotic bodies. To detect the apoptosis of nematodes, nematodes exposed to PS-NPs for 72 h were incubated with AO (2 μg/mL) in K^+ medium for 2 h in the dark. Then, nematodes were anesthetized with levamisole solution (60 μm), photographed with a microscope (Olympus BX51, Japan), and analyzed with ImageJ software.[50]

4.9. Real Time-Quantitative Polymerase Chain Reaction. After exposure, nematodes were washed three times with K medium, and then, TRIzol reagents were applied to extract total RNA. The quality and concentration of RNA were measured with a NanoDrop ND-2000 spectrophotometer (Agilent technology, US). RNA with a 1.8−2.0 value of OD260/OD280 was used to reversely transcribe cDNA according to the protocol of the Fast Quant cDNA kit. Subsequently, target genes were amplified with the StepOnePlus RT-qPCR kit.[54] The PCR primers shown in Table 2 were synthesized and purchased from Generay (Shanghai, China). The expressions of target genes were quantified using the $\Delta\Delta C_t$ method and normalized to internal reference actin. For every gene, three replicates were set up for each treatment condition group.

Table 2. Primer Sequences for RT-qPCR

gene name	primer	primer sequence (5′−3′)
sel-12	forward	AGACAGTATCGTTGAGAAGG
	reverse	AAGACCAGAGCCATTAGTG
hop-1	forward	GCCAGAACAACAAGAACAAT
	reverse	GTCAGAACAGCAACAATATCC
actin	forward	GGCATCACACCTTCTACA
	reverse	TGACACCATCTCCAGAGT

4.10. Statistical Analysis. Data were expressed in the form of arithmetic mean ± standard deviation (mean ± SD) and analyzed using SPSS (13.0) software. Experimental image data were analyzed using ImageJ software. The data results among groups were compared by one-way ANOVA with the Post Hoc test. A p value less than 0.05 was considered to be statistically significant.

AUTHOR INFORMATION

Corresponding Authors

Yan Han − *Department of Neurology, Yueyang Hospital of Integrated Traditional Chinese and Western Medicine, Shanghai University of Traditional Chinese Medicine, Shanghai 200437, China*; Email: hanyan.2006@aliyun.com.cn

Mingyuan Liu − *Department of Neurology, Yueyang Hospital of Integrated Traditional Chinese and Western Medicine, Shanghai University of Traditional Chinese Medicine, Shanghai 200437, China*; orcid.org/0000-0002-1952-1012; Email: mingyuan.liu@foxmail.com.cn

Authors

Qianyun Liu − *Department of Neurology, Yueyang Hospital of Integrated Traditional Chinese and Western Medicine,*

https://dx.doi.org/10.1021/acsomega.0c04830
ACS Omega 2020, 5, 33170−33177

Shanghai University of Traditional Chinese Medicine, Shanghai 200437, China

Chunxiang Chen − *Shanghai University of Traditional Chinese Medicine, Shanghai 201203, China*

Mengting Li − *Shanghai University of Traditional Chinese Medicine, Shanghai 201203, China*

Jia Ke − *Shanghai University of Traditional Chinese Medicine, Shanghai 201203, China*

Yichen Huang − *Shanghai University of Traditional Chinese Medicine, Shanghai 201203, China*

Yuefeng Bian − *Shanghai University of Traditional Chinese Medicine, Shanghai 201203, China*

Shufen Guo − *Shanghai University of Traditional Chinese Medicine, Shanghai 201203, China*

Yang Wu − *Shanghai University of Traditional Chinese Medicine, Shanghai 201203, China*

Complete contact information is available at: https://pubs.acs.org/10.1021/acsomega.0c04830

Author Contributions

[§]Q.L. and C.C. contributed equally to this work.

Notes

The authors declare no competing financial interest.

■ ACKNOWLEDGMENTS

This work was supported by the National Key Research and Development Program of China (no. 2019YFC1711603) and the National Natural Science Foundation of China (nos 81771288 and 81771303). This work was also supported by the Shanghai Pujiang Program (no. 17PJ1411000).

■ REFERENCES

(1) Bouwmeester, H.; Hollman, P. C. H.; Peters, R. J. B. Potential Health Impact of Environmentally Released Micro- and Nanoplastics in the Human Food Production Chain: Experiences from Nanotoxicology. *Environ. Sci. Technol.* **2015**, *49*, 8932−8947.

(2) Lehner, R.; Weder, C.; Petri-Fink, A.; Rothen-Rutishauser, B. Emergence of Nanoplastic in the Environment and Possible Impact on Human Health. *Environ. Sci. Technol.* **2019**, *53*, 1748−1765.

(3) Neves, D.; Sobral, P.; Ferreira, J. L.; Pereira, T. Ingestion of microplastics by commercial fish off the Portuguese coast. *Mar. Pollut. Bull.* **2015**, *101*, 119−126.

(4) Zhao, S.; Zhu, L.; Li, D. Microscopic anthropogenic litter in terrestrial birds from Shanghai, China: Not only plastics but also natural fibers. *Sci. Total Environ.* **2016**, *550*, 1110−1115.

(5) Lenz, R.; Enders, K.; Nielsen, T. G. Microplastic exposure studies should be environmentally realistic. *Proc. Natl. Acad. Sci. U. S. A.* **2016**, *113*, E4121−E4122.

(6) Acosta-Coley, I.; Mendez-Cuadro, D.; Rodriguez-Cavallo, E.; de la Rosa, J.; Olivero-Verbel, J. Trace elements in microplastics in Cartagena: A hotspot for plastic pollution at the Caribbean. *Mar. Pollut. Bull.* **2019**, *139*, 402−411.

(7) De-la-Torre, G. E. Microplastics: an emerging threat to food security and human health. *J. Food Sci. Technol.* **2020**, *57*, 1601−1608.

(8) Prata, J. C.; da Costa, J. P.; Lopes, I.; Duarte, A. C.; Rocha-Santos, T. Environmental exposure to microplastics: An overview on possible human health effects. *Sci. Total Environ.* **2020**, *702*, 134455.

(9) Jani, P.; Halbert, G. W.; Langridge, J.; Florence, A. T. Nanoparticle uptake by the rat gastrointestinal mucosa: quantitation and particle size dependency. *J. Pharm. Pharmacol.* **1990**, *42*, 821−826.

(10) Schwabl, P.; Köppel, S.; Königshofer, P.; Bucsics, T.; Trauner, M.; Reiberger, T.; Liebmann, B. Detection of Various Microplastics in Human Stool: A Prospective Case Series. *Ann. Intern. Med.* **2019**, *171*, 453−457.

(11) Ding, J.; Huang, Y.; Liu, S.; Zhang, S.; Zou, H.; Wang, Z.; Zhu, W.; Geng, J. Toxicological effects of nano- and micro-polystyrene plastics on red tilapia: Are larger plastic particles more harmless? *J. Hazard. Mater.* **2020**, *396*, 122693.

(12) Ding, J.; Zhang, S.; Razanajatovo, R. M.; Zou, H.; Zhu, W. Accumulation, tissue distribution, and biochemical effects of polystyrene microplastics in the freshwater fish red tilapia (Oreochromis niloticus). *Environ. Pollut.* **2018**, *238*, 1−9.

(13) Prüst, M.; Meijer, J.; Westerink, R. The plastic brain: neurotoxicity of micro- and nanoplastics. *Part. Fibre Toxicol.* **2020**, *17*, 24.

(14) Teleanu, D.; Chircov, C.; Grumezescu, A.; Teleanu, R. Neurotoxicity of Nanomaterials: An Up-to-Date Overview. *Nanomaterials* **2019**, *9*, 96.

(15) Barboza, L. G. A.; Vieira, L. R.; Branco, V.; Figueiredo, N.; Carvalho, F.; Carvalho, C.; Guilhermino, L. Microplastics cause neurotoxicity, oxidative damage and energy-related changes and interact with the bioaccumulation of mercury in the European seabass, Dicentrarchus labrax (Linnaeus, 1758). *Aquat. Toxicol.* **2018**, *195*, 49−57.

(16) Avio, C. G.; Gorbi, S.; Milan, M.; Benedetti, M.; Fattorini, D.; d'Errico, G.; Pauletto, M.; Bargelloni, L.; Regoli, F. Pollutants bioavailability and toxicological risk from microplastics to marine mussels. *Environ. Pollut.* **2015**, *198*, 211−222.

(17) Deng, Y.; Zhang, Y.; Lemos, B.; Ren, H. Tissue accumulation of microplastics in mice and biomarker responses suggest widespread health risks of exposure. *Sci. Rep.* **2017**, *7*, 46687.

(18) Browne, M. A.; Dissanayake, A.; Galloway, T. S.; Lowe, D. M.; Thompson, R. C. Ingested microscopic plastic translocates to the circulatory system of the mussel, Mytilus edulis (L). *Environ. Sci. Technol.* **2008**, *42*, 5026−5031.

(19) Varó, I.; Perini, A.; Torreblanca, A.; Garcia, Y.; Bergami, E.; Vannuccini, M. L.; Corsi, I. Time-dependent effects of polystyrene nanoparticles in brine shrimp Artemia franciscana at physiological, biochemical and molecular levels. *Sci. Total Environ.* **2019**, *675*, 570−580.

(20) Chen, Q.; Yin, D.; Jia, Y.; Schiwy, S.; Legradi, J.; Yang, S.; Hollert, H. Enhanced uptake of BPA in the presence of nanoplastics can lead to neurotoxic effects in adult zebrafish. *Sci. Total Environ.* **2017**, *609*, 1312−1321.

(21) Mattsson, K.; Johnson, E.; Malmendal, A.; Linse, S.; Hansson, L.; Cedervall, T. Brain damage and behavioural disorders in fish induced by plastic nanoparticles delivered through the food chain. *Sci. Rep.* **2017**, *7*, 11452.

(22) Li, Z.; Feng, C.; Wu, Y.; Guo, X. Impacts of nanoplastics on bivalve: Fluorescence tracing of organ accumulation, oxidative stress and damage. *J. Hazard. Mater.* **2020**, *392*, 122418.

(23) Sarasamma, S.; Audira, G.; Siregar, P.; Malhotra, N.; Lai, Y.; Liang, S.; Chen, J.; Chen, K.; Hsiao, C. Nanoplastics Cause Neurobehavioral Impairments, Reproductive and Oxidative Damages, and Biomarker Responses in Zebrafish: Throwing up Alarms of Wide Spread Health Risk of Exposure. *Int. J. Mol. Sci.* **2020**, *21*, 1410.

(24) Leung, M. C. K.; Williams, P. L.; Benedetto, A.; Au, C.; Helmcke, K. J.; Aschner, M.; Meyer, J. N. Caenorhabditis elegans: an emerging model in biomedical and environmental toxicology. *Toxicol. Sci.* **2008**, *106*, 5−28.

(25) Shaye, D. D.; Greenwald, I. OrthoList: a compendium of C. elegans genes with human orthologs. *PLoS One* **2011**, *6*, No. e20085.

(26) Hamada, T.; Morita, M.; Miyakawa, M.; Sugimoto, R.; Hatanaka, A.; Vestergaard, M. d. C.; Takagi, M. Size-dependent partitioning of nano/microparticles mediated by membrane lateral heterogeneity. *J. Am. Chem. Soc.* **2012**, *134*, 13990−13996.

(27) Lei, L.; Liu, M.; Song, Y.; Lu, S.; Hu, J.; Cao, C.; Xie, B.; Shi, H.; He, D. Polystyrene (nano)microplastics cause size-dependent neurotoxicity, oxidative damage and other adverse effects in Caenorhabditis elegans. *Environ. Sci.: Nano* **2018**, *5*, 2009−2020.

(28) Zhao, T.; Tan, L.; Zhu, X.; Huang, W.; Wang, J. Size-dependent oxidative stress effect of nano/micro-scaled polystyrene on Karenia mikimotoi. *Mar. Pollut. Bull.* **2020**, *154*, 111074.

(29) Chalorak, P.; Jattujan, P.; Nobsathian, S.; Poomtong, T.; Sobhon, P.; Meemon, K. Holothuria scabra extracts exhibit anti-Parkinson potential in C. elegans: A model for anti-Parkinson testing. *Nutr. Neurosci.* **2018**, *21*, 427−438.
(30) Magni, S.; Gagné, F.; André, C.; Della Torre, C.; Auclair, J.; Hanana, H.; Parenti, C. C.; Bonasoro, F.; Binelli, A. Evaluation of uptake and chronic toxicity of virgin polystyrene microbeads in freshwater zebra mussel Dreissena polymorpha (Mollusca: Bivalvia). *Sci. Total Environ.* **2018**, *631−632*, 778−788.
(31) Hoelting, L.; Scheinhardt, B.; Bondarenko, O.; Schildknecht, S.; Kapitza, M.; Tanavde, V.; Tan, B.; Lee, Q. Y.; Mecking, S.; Leist, M.; Kadereit, S. A 3-dimensional human embryonic stem cell (hESC)-derived model to detect developmental neurotoxicity of nanoparticles. *Arch. Toxicol.* **2013**, *87*, 721−733.
(32) Burbulla, L. F.; Song, P.; Mazzulli, J. R.; Zampese, E.; Wong, Y. C.; Jeon, S.; Santos, D. P.; Blanz, J.; Obermaier, C. D.; Strojny, C.; Savas, J. N.; Kiskinis, E.; Zhuang, X.; Krüger, R.; Surmeier, D. J.; Krainc, D. Dopamine oxidation mediates mitochondrial and lysosomal dysfunction in Parkinson's disease. *Science* **2017**, *357*, 1255−1261.
(33) Xia, T.; Kovochich, M.; Liong, M.; Zink, J. I.; Nel, A. E. Cationic polystyrene nanosphere toxicity depends on cell-specific endocytic and mitochondrial injury pathways. *ACS Nano* **2008**, *2*, 85−96.
(34) Ruenraroengsak, P.; Tetley, T. Differential bioreactivity of neutral, cationic and anionic polystyrene nanoparticles with cells from the human alveolar compartment: robust response of alveolar type 1 epithelial cells. *Part. Fibre Toxicol.* **2015**, *12*, 19.
(35) Ribeiro, F.; Garcia, A. R.; Pereira, B. P.; Fonseca, M.; Mestre, N. C.; Fonseca, T. G.; Ilharco, L. M.; Bebianno, M. J. Microplastics effects in Scrobicularia plana. *Mar. Pollut. Bull.* **2017**, *122*, 379−391.
(36) Kim, S. W.; Kwak, J. I.; An, Y.-J. Multigenerational study of gold nanoparticles in Caenorhabditis elegans: transgenerational effect of maternal exposure. *Environ. Sci. Technol.* **2013**, *47*, 5393−5399.
(37) Qu, M.; Qiu, Y.; Kong, Y.; Wang, D. Amino modification enhances reproductive toxicity of nanopolystyrene on gonad development and reproductive capacity in nematode Caenorhabditis elegans. *Environ. Pollut.* **2019**, *254*, 112978.
(38) Wang, F.; Bexiga, M. G.; Anguissola, S.; Boya, P.; Simpson, J. C.; Salvati, A.; Dawson, K. A. Time resolved study of cell death mechanisms induced by amine-modified polystyrene nanoparticles. *Nanoscale* **2013**, *5*, 10868−10876.
(39) Fröhlich, E.; Meindl, C.; Roblegg, E.; Ebner, B.; Absenger, M.; Pieber, T. R. Action of polystyrene nanoparticles of different sizes on lysosomal function and integrity. *Part. Fibre Toxicol.* **2012**, *9*, 26.
(40) Stone, V.; Miller, M. R.; Clift, M. J. D.; Elder, A.; Mills, N. L.; Møller, P.; Schins, R. P. F.; Vogel, U.; Kreyling, W. G.; Alstrup Jensen, K.; Kuhlbusch, T. A. J.; Schwarze, P. E.; Hoet, P.; Pietroiusti, A.; De Vizcaya-Ruiz, A.; Baeza-Squiban, A.; Teixeira, J. P.; Tran, C. L.; Cassee, F. R. Nanomaterials Versus Ambient Ultrafine Particles: An Opportunity to Exchange Toxicology Knowledge. *Environ. Health Perspect.* **2017**, *125*, 106002.
(41) Ankarcrona, M.; Hultenby, K. Presenilin-1 is located in rat mitochondria. *Biochem. Biophys. Res. Commun.* **2002**, *295*, 766−770.
(42) Area-Gomez, E.; Del Carmen Lara Castillo, M.; Tambini, M. D.; Guardia-Laguarta, C.; de Groof, A. J. C.; Madra, M.; Ikenouchi, J.; Umeda, M.; Bird, T. D.; Sturley, S. L.; Schon, E. A. Upregulated function of mitochondria-associated ER membranes in Alzheimer disease. *EMBO J.* **2012**, *31*, 4106−4123.
(43) Wüst, R.; Maurer, B.; Hauser, K.; Woitalla, D.; Sharma, M.; Krüger, R. Mutation analyses and association studies to assess the role of the presenilin-associated rhomboid-like gene in Parkinson's disease. *Neurobiol. Aging* **2016**, *39*, 217.e13.
(44) Agarwal, I.; Farnow, C.; Jiang, J.; Kim, K.-S.; Leet, D. E.; Solomon, R. Z.; Hale, V. A.; Goutte, C. HOP-1 Presenilin Deficiency Causes a Late-Onset Notch Signaling Phenotype That Affects Adult Germline Function in Caenorhabditis elegans. *Genetics* **2018**, *208*, 745−762.
(45) Kitagawa, N.; Shimohama, S.; Oeda, T.; Uemura, K.; Kohno, R.; Kuzuya, A.; Shibasaki, H.; Ishii, N. The role of the presenilin-1 homologue gene sel-12 of Caenorhabditis elegans in apoptotic activities. *J. Biol. Chem.* **2003**, *278*, 12130−12134.
(46) Wu, S.; Lei, L.; Song, Y.; Liu, M.; Lu, S.; Lou, D.; Shi, Y.; Wang, Z.; He, D. Mutation of hop-1 and pink-1 attenuates vulnerability of neurotoxicity in C. elegans: the role of mitochondria-associated membrane proteins in Parkinsonism. *Exp. Neurol.* **2018**, *309*, 67−78.
(47) Xiao, X.; Zhang, X.; Zhang, C.; Li, J.; Zhao, Y.; Zhu, Y.; Zhang, J.; Zhou, X. Toxicity and multigenerational effects of bisphenol S exposure to Caenorhabditis elegans on developmental, biochemical, reproductive and oxidative stress. *Toxicol. Res.* **2019**, *8*, 630−640.
(48) Wang, X.; Zhang, L.; Zhang, L.; Wang, W.; Wei, S.; Wang, J.; Che, H.; Zhang, Y. Effects of excess sugars and lipids on the growth and development of Caenorhabditis elegans. *Genes Nutr.* **2020**, *15*, 1.
(49) Xu, T.; Li, P.; Wu, S.; Lei, L.; He, D. Tris(2-chloroethyl) phosphate (TCEP) and tris(2-chloropropyl) phosphate (TCPP) induce locomotor deficits and dopaminergic degeneration in Caenorhabditis elegans. *Toxicol Res.* **2017**, *6*, 63−72.
(50) Pincus, Z.; Slack, F. Developmental biomarkers of aging in Caenorhabditis elegans. *Dev. Dyn.* **2010**, *239*, 1306−1314.
(51) Yan, Q.; Zhao, R.; Zheng, W.; Yin, C.; Zhang, B.; Ma, W. Generation of an external guide sequence library for a reverse genetic screen in Caenorhabditis elegans. *BMC Biotechnol.* **2009**, *9*, 47.
(52) Burchfield, S. L.; Bailey, D. C.; Todt, C. E.; Denney, R. D.; Negga, R.; Fitsanakis, V. A. Acute exposure to a glyphosate-containing herbicide formulation inhibits Complex II and increases hydrogen peroxide in the model organism Caenorhabditis elegans. *Environ. Toxicol. Pharmacol.* **2019**, *66*, 36−42.
(53) Kim, H. M.; Long, N. P.; Yoon, S. J.; Nguyen, H. T.; Kwon, S. W. Metabolomics and phenotype assessment reveal cellular toxicity of triclosan in Caenorhabditis elegans. *Chemosphere* **2019**, *236*, 124306.
(54) Wang, C.; An, J.; Bai, Y.; Li, H.; Chen, H.; Ou, D.; Liu, Y. Tris(1,3-dichloro-2-propyl) phosphate accelerated the aging process induced by the 4-hydroxynon-2-enal response to reactive oxidative species in Caenorhabditis elegans. *Environ. Pollut.* **2019**, *246*, 904−913.

https://dx.doi.org/10.1021/acsomega.0c04830
ACS Omega 2020, 5, 33170−33177